

PROPAGATION OF TOPOGRAPHICALLY GENERATED INTERNAL WAVES IN THE ATMOSPHERE

JULIE C. VANDERHOFF *

Brigham Young University, Provo, Utah

ABSTRACT

The propagation of small-scale internal gravity wave packets through large-scale inertial frequency waves is investigated through ray theory and numerically solving the fully non-linear Navier-Stokes equations in two dimensions. Small-scale internal waves generated by flow over topography interact with both time-independent background shear profiles and time-dependent shears present in the atmosphere in the form of large-scale waves of inertial frequency propagating upward. Interaction with a time-independent shear may lead to a critical layer interaction and eventual short wave absorption or breaking. When the shear is time-dependent and the energy of both the small- and large-scale waves are propagating in the same direction, a critical layer may be approached, but because of the time-dependent nature of the background it may disappear before the small-scale wave is absorbed or breaks. Although both numerical and observational studies have been performed to address this issue, the details of this type interaction are not fully understood, and seem to be highly sensitive to initial wave parameters and location. Through ray theory many small-scale waves can be traced, and data collected on the evolution of their energy and propensity to break. An investigation of many small-scale waves with a range of realistic initial wave parameters and vertical locations propagating upward through an upward propagating inertial wave give insight into the propagation of terrain generated internal waves through a time-dependent background flow, and result in a classification of probable types of short wave interactions.

1. Introduction

Internal waves are ubiquitous throughout the atmosphere. Strong generation regions in the stratosphere, such as mountain ranges, can generate a stream of internal waves propagating upward into the middle atmosphere. Internal waves may also be generated through convection, wind shear, adjustment of unbalanced flows near jet streams and frontal systems, and body forcing accompanying localized wave dissipation (Fritts and Alexander (2003)). These small-scale gravity waves may interact with other waves, winds, and the changing buoyancy frequency as they propagate. Each of these interactions, in addition to gravity wave dissipation, may contribute to the universal frequency spectrum, slopes near $-5/4$, seen in the middle atmosphere (VanZandt (1982), Balsley and Carter (1982), Nakamura, Tsuda, Fukao, Kato, Manson, and Meek (1993), Collins, Nomura, and Gardner (1994)). The importance of each of these individual effects is unknown and the resulting spectral shapes and wave

breaking are not well understood (Gardner (1996)).

The location of wave-breaking and dissipation is important to understanding the combined effect a number of small-scale gravity waves can have on the atmosphere, including their influence on large-scale circulation. Some examples of gravity-wave-driven features are the quasi-biennial oscillation of the equatorial lower stratosphere (Takahashi, Zhao, and Kumakura (1997)), the semiannual oscillations of the equatorial upper stratosphere and mesosphere (Hamilton and Mahlman (1988)), the annual mesospheric meridional circulation, and the separated winter stratopause (Hitchman, Gille, Rodgers, and Grasseur (1989)). These effects are important to include in global circulation models (GCMs), but the internal gravity waves which generate them cannot be resolved. Parameterization of the generation and evolution of internal gravity wave activity through the atmosphere is necessary for accurate GCMs.

Ray theory has been used as a method to parameterize gravity wave propagation through steady background winds as well as with tidal winds present (Zhong, Sonmor, Manson, and Meek (1995)). With only steady background shear present, vertical wave-

*Corresponding author address: Julie C. Vanderhoff, Mechanical Engineering Department, Brigham Young University, 435 CTB, Provo, UT, 84602-4201. (email: jvanderhoff@byu.edu).

length cutoff values have been prescribed assuming wave-breaking and dissipation will occur for waves reaching these small scales (Henyey, Wright, and Flatté (1986)). Although this may be accurate for steady shear profiles, Eckermann (1997) found allowing for time-dependent shear profiles results in small-scale internal wave propagation which is very different from steady profiles. Depending on the relative motion of the time-dependent shear, the short waves may reach caustics (Broutman, Macaskill, McIntyre, and Rottman (1997), Vanderhoff, Nomura, Rottman, and Macaskill (2008), Sonmor and Klaasen (2000)) which only occur due to the time-dependence, or unsteady critical layers (Sartelet (2003a,b)). Also prevalent in the atmosphere are inertial scale waves propagating upward, which can be modeled as stationary time-dependent shears, where the phases of the inertial wave propagate downward. These interactions with low frequency motions may cause Doppler-spreading of the short waves or possibly even breaking.

We assume strong internal gravity wave generation by the mountains in Whistler, B.C., Canada. These upward propagating small-scale waves may interact with strong background steady shear in addition to other, larger-scale, inertial frequency waves. The interactions between these waves will define which small-scale waves will continue to propagate upwards and contribute to internal wave activity in the mesosphere, which will have a change in their properties, and which will break.

In the next section, background information on the idealized problem and solution methods, ray tracing, and numerical simulations, is presented. In Section 3 the results of small-scale wave propagation through different mediums is addressed for both ray tracing and numerical simulations. Conclusions are drawn in Section 4.

2. Setup

In this section we will cover the different setups of the ray tracing calculations and numerical simulations.

a. The idealized problem

In the ray tracing and numerical simulations we consider the case of a packet of short waves approaching a single inertia packet either from above or below, as described in Vanderhoff, Nomura, Rottman, and Macaskill (2008), where a steady shear may be present as well. The coordinate system is (x, y, z) with z positive upwards, x positive eastward, and y positive northward. We assume that the buoyancy frequency N and the Coriolis parameter f are both constant.

The inertial packet has wavenumber $\mathbf{K} = (0, 0, M)$, where $M = 2\pi/\lambda_i$ and λ_i is the vertical wavelength of the wave. The corresponding velocity field is uniform, horizontally, $\mathbf{u} = (u, v, 0)$, but confined in the vertical by a Gaussian envelope:

$$U + iV = U_0 e^{-z^2/L^2} e^{i(Mz-ft)} \quad (1)$$

where L and U_0 are constants, real and complex respectively. The envelope of the inertia-wave packet assumed stationary, since the vertical component of the group velocity vanishes at the inertial frequency. The phases move vertically through the packet at speed $c = f/M$, assumed positive for the moment. A steady shear may be superimposed on the background with a linear profile seen in the stratosphere, which increases with height or the mesosphere which decreases with height. In the numerical simulations we use a gaussian profile with a maximum horizontal velocity of 50m/s,

$$U_{steady} = U_{max} e^{-z^2/L^2} . \quad (2)$$

Waves propagating to the east which do not reach a critical level while in a background velocity going to the east will not change while going back through the opposite shear as they propagate upwards. Therefore we will concentrate on short waves which reach a critical level or turning point during the first strong shear interaction.

The short waves have wavenumber $\mathbf{k} = (k, 0, m)$, with k constant, and intrinsic frequency $\hat{\omega}$, which is the Doppler-shifted frequency, where

$$\hat{\omega}^2 = (N^2 k^2 + f^2 m^2)/(k^2 + m^2) \quad (3)$$

which simplifies to

$$\hat{\omega}^2 \approx \frac{N^2 k^2}{m^2} \quad (4)$$

when $f^2 \ll \hat{\omega}^2 \ll N^2$. We take m and $\hat{\omega}$ to be positive, and allow k to have either sign. The vertical group velocity $c_g = \partial\hat{\omega}/\partial m$ is negative if m is positive and positive if m is negative.

The vertical displacement of the short waves is $\zeta = \zeta_0 \exp(i\theta)$, from which the wavenumber and wave frequency are given by $\mathbf{k} = \nabla\theta$ and $\omega = -\theta_t$, respectively, and where $\omega = \hat{\omega} + kU$. The wave-energy density E is related to ζ_0 by

$$E = \frac{1}{2} \rho_0 \zeta_0^2 N^2 \left[1 + \left(\frac{fm}{Nk} \right)^2 \right] \quad (5)$$

where ρ_0 is the mean density of the fluid.

The numerical simulations are initialized at time $t = 0$ with a short-wave packet whose vertical displacement field $\zeta(x, z, t)$ has the initial form

$$\zeta(x, z, 0) = \text{Re} \left\{ \zeta_0 e^{-(z-z_0)^2/\ell^2} e^{i(kx+mz)} \right\} \quad (6)$$

where ℓ and z_0 are real constants and ζ_0 is a complex constant. The initial vertical position z_0 is specified such that the short-wave packet is below the inertia-wave packet since $c_g > 0$.

Wave-breaking is defined when isopycnals are vertical, $\zeta_z > 1$, leading to overturning within the fluid and resulting turbulence. This can be calculated in the numerical simulations by finding $\Delta\zeta/\Delta z$. For calculating wave steepness in ray theory we use the dispersion relation and (5) to derive:

$$\zeta_z = -m \left| \left(\frac{2A\hat{\omega}}{\rho_0} \right)^{1/2} N^{-1} \right|. \quad (7)$$

Here $A = E/\hat{\omega}$ is the wave-action density. There is an inverse relationship between the wave steepness and the Richardson number, where $Ri = N^2/u_z^2$, which is:

$$Ri = \frac{1 - f^2/\hat{\omega}^2}{\zeta_z^2}. \quad (8)$$

For the ray tracing and numerical simulation results shown in this paper, we use the following atmospheric parameters, which are within the range of internal waves in the stratosphere and mesosphere at the latitude of Whistler, B.C., CA: $M = 2\pi/(10000 \text{ m})$, $k = 2\pi/(10000 \text{ m})$, $f = 1.114 \times 10^{-4} \text{ s}^{-1}$, $N = 0.02 \text{ s}^{-1}$, and $U_0 = 10 \text{ m/s}$ for the inertial wave and $U_{max} = 50 \text{ m/s}$ for the shear profiles. For the numerical simulations, the initial steepness $|\zeta_z| = |m\zeta_0| = 0.1$, where subscript z represents the partial derivative with respect to z , $ML = 16$, and $\ell/L = 0.6$. We will alter the vertical wavenumber, m , to realize different group speeds of the short wave. The vertical wavelength never exceeds 30km so the change in background density over a wavelength is not significant in the calculations.

b. Ray Theory

Using ray theory we can calculate approximately the behavior of the short wave encounter with the inertial wave group. To do this we assume that the inertial wave is both unaffected by the short wave interaction and has a much larger length scale than that of the short wave. Also we assume the short wave is determined by the linear dispersion relation. Then an evolution equation in characteristic form can be found for \mathbf{k} . For further detail see Vanderhoff et al. (2008).

1) THE RAY EQUATIONS

The ray-tracing results in this paper are obtained with the following pair of ray equations, for the vertical position of the ray path and the vertical wavenumber respectively:

$$\frac{d\mathbf{x}}{dt} = c_g + \mathbf{U}, \quad \frac{dm}{dt} = -k \frac{\partial u}{\partial z}. \quad (9)$$

Here $d/dt = \partial/\partial t + c_g \bullet \nabla$. Because the expression (1) has no dependence on x or y , the horizontal components $(k, 0)$ of the wavenumber of the short waves are conserved along the ray. These equations are solved using the Matlab ODE45 solver which is based on an explicit Runge-Kutta formula, the Dormand-Prince pair, Dormand and Prince (1980), which is a one-step solver. The tolerances are set at 10^{-4} for the relative error and 10^{-6} for the absolute error.

2) ANALYTIC RAY SOLUTIONS

An analytic ray solution describing short-wave refraction by inertia waves propagating opposite to the small scale waves appears in Broutman and Young (1986) and is obtained by letting L approach infinity in equation (1). The inertia-wave velocity \mathbf{U} is then purely sinusoidal. In a reference frame moving at the inertial-wave phase speed c , the inertial current appears steady. Solutions then exist for which the short-wave frequency in the inertial-wave reference frame

$$\Omega = \hat{\omega} + kU - cm \approx \text{constant}. \quad (10)$$

When the vertical group speed of the short wave is in the same direction as the inertial wave the result is transient critical levels. A critical level occurs when the relative frequency of the internal wave tends to zero, $\hat{\omega} = 0$, such that oscillations relative to the background wind cease, which for a steady background is

$$\Omega = kU. \quad (11)$$

This occurs where the horizontal phase speed of the internal wave is equal to the horizontal velocity of the background,

$$U = \Omega/k = c_{px}. \quad (12)$$

In a steady shear profile if a critical level is present, the short wave is eventually absorbed by the mean flow, or may be transmitted or reflected depending on the amplitude of the incident wave. When an inertial wave is present

$$\Omega = kU - cm. \quad (13)$$

With a short wave vertical wavelength of only 1000m and an inertial wave where $U_{max} = 10 \text{ m/s}$ the second term on the right hand side is an order of magnitude less than that on the right. This disparity increases

as the vertical wavelength increases and the horizontal background velocity increases. Thus this term is neglected and the approach to a critical level is expected as is calculated for steady flows. When short waves are traveling upward through the inertial wave the value of the horizontal phase speed at the critical level is merely a different sign if the wave is traveling in the positive or negative x -direction. If k is positive (short wave traveling in positive x -direction, here traveling to the east) and m is negative (short wave traveling upward), the value of the background velocity at the critical level is positive, and for upward, west traveling waves, the background velocity at the critical level is also to the west.

If the horizontal wave propagation is opposite to the steady horizontal velocity turning points may ensue. A turning point is where the intrinsic frequency of the short wave approaches the buoyancy frequency,

$$\Omega = N + Uk - cm, \quad (14)$$

above which it cannot propagate. Again the cm term is very small for larger scale waves and the interaction approaches that of a steady shear profile,

$$\Omega = N + kU. \quad (15)$$

This occurs when the horizontal group speed of the short wave is equal to the negative horizontal background velocity. At the turning point the rays become horizontal and can only turn back on themselves. The short wave vertical group speed passes through zero and changes sign, the horizontal group speed approaches zero, but then goes negative again.

When the short waves are propagating opposite to the inertial wave caustic interactions occur. For our idealized model, caustics occur when

$$c_g = c. \quad (16)$$

Vanderhoff et al. (2008) show results for these types of interactions. These types of interactions are less likely to occur in the atmosphere with most internal waves having upward group speeds.

c. Numerical Simulations

Numerical results are obtained by integrating the fully nonlinear inviscid, Boussinesq equations of motion. In their vorticity-streamfunction form, these are:

$$\frac{\partial^2 \psi}{\partial x^2} + \frac{\partial^2 \psi}{\partial z^2} = q \quad (17)$$

$$\frac{\partial q}{\partial t} - J(\psi, q) - \frac{\partial \sigma}{\partial x} - f \frac{\partial v}{\partial z} = 0 \quad (18)$$

$$\frac{\partial v}{\partial t} - J(\psi, v) + fu = 0 \quad (19)$$

$$\frac{\partial \sigma}{\partial t} - J(\psi, \sigma) - N^2 w = 0, \quad (20)$$

where q is the y -component of vorticity and $J(\psi, q)$ the Jacobian with respect to (x, z) . Here the fluid velocity $\mathbf{u} = (u, v, w)$, and the stream function ψ is defined such that $u = \partial\psi/\partial z$, $w = -\partial\psi/\partial x$, and $q = \partial u/\partial z - \partial w/\partial x$. The scaled density perturbation due to the presence of internal wave motions is $\sigma = g\rho'/\rho_0$ where g is the acceleration due to gravity; the density $\rho = \rho' + \rho_0$, with $\rho_0(z)$ the mean density profile. Because of rotation, there is a nonzero v field, but all variables are assumed to be independent of y . The scale height is not included because the relatively small vertical scale of the waves results in insignificant changes in density over the height of the wave.

Periodic boundary conditions are imposed in both the x - and z -directions, and the equations are solved using a Fourier spectral collocation technique with Runge-Kutta time stepping. The computational domain contains one horizontal wavelength of the short waves in the horizontal direction and one vertical wavelength of the inertia waves in the vertical direction.

There are 512 grid points in the vertical direction, but only 16 grid points in the horizontal direction. The low horizontal resolution suffices for this problem – as has been verified by tests at higher resolution – because the short waves, though strongly refracted, are not strongly amplified, and remain well below breaking threshold. The maximum wave-steepness $\partial\zeta/\partial z$ of the short waves over the duration of the simulation does not exceed unity (except in a special case as discussed later). No viscosity or filtering was necessary to stabilize the calculations.

3. Results

a. Ray Tracing through an inertial wave

The ray path of a short wave with horizontal phase speed of 5m/s propagating upward through a stationary inertial wave with phases propagating downward is shown in Fig.1. Critical levels are approached as the phases propagate through but then the small-scale internal waves propagate back to their original properties as the critical level propagates through. The $x - z$

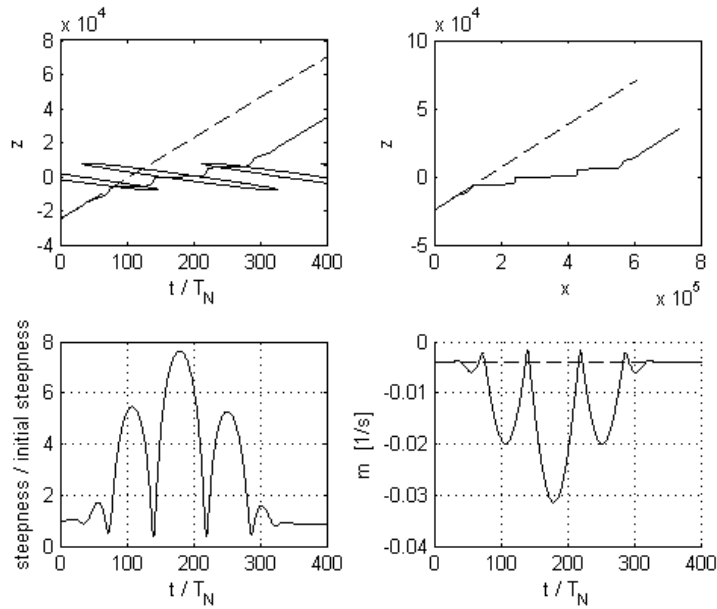


FIG. 1. Short wave with horizontal phase speed 5m/s. Solid line is ray path interacting with inertial wave, dashed line is path with no inertial wave present. The upper left plot is the ray path where the elliptical regions are outlines of critical layer values. As the ray flattens out in $z - t$ space it is approaching a critical layer, where the longest time it does so is in the largest part of the envelope. Upper right plot is ray path in $x - z$ space, lower left plot is the steepness of the short wave during the interaction, where it increases as approaching a critical layer, then drops as the critical layer propagates through. The lower right plot is the change in vertical wavenumber over the ray.

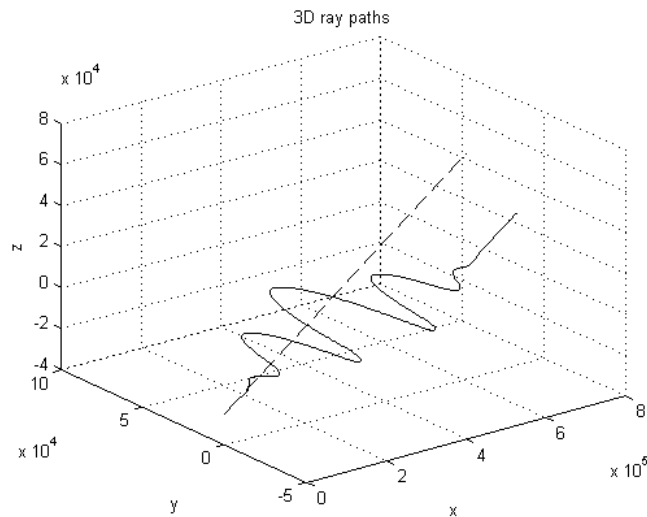


FIG. 2. Short wave with horizontal phase speed 5m/s. Ray path in $x - y - z$ space. Solid line is ray path interacting with inertial wave, dashed line is path with no inertial wave present. Oscillations in y -direction are due to the inertial wave oscillations. Ray exits interaction with approximately the same properties it entered with.

space plot shows the increased horizontal distance the short wave travels as it approaches a critical level due to the inertial wave interaction. If no inertial wave were present, dashed line, at the final height the wave is approximately 150 km west of its current location. So although the final short wave properties are not irreversibly altered, their horizontal location can be shifted hundreds of kilometers. As the short wave approaches the critical level its steepness increases, and may break if the initial steepness is great enough, but if not it will drop back to its initial steepness. In this case if $U_0 = 13\text{m/s}$ the steepness would be greater than unity for a few time steps. This corresponds to short wave breaking when:

$$U = c_{px0} + \frac{c}{k}(m_0 - m_{break}) \quad (21)$$

where

$$\frac{\zeta_z}{\zeta_{z0}} = 10 = \frac{m_{break}}{m_0} \frac{(1 + \frac{fm_{break}}{(Nk)^2})^{1/2}}{(1 + \frac{fm_0}{(Nk)^2})^{1/2}}, \quad (22)$$

which was derived using equation 13. This is only true for a small range of values and the resulting phenomenon is currently being explored further.

The vertical wavenumber increases just as the critical level is approached and after it passes, in between it decreases. There is no net change in vertical wavenumber, however, and thus there is also no net change in the energy of the short waves.

$$\int EdV = \int A\hat{\omega}dV \quad (23)$$

where V is the volume of the short wave packet. Due to wave action conservation, $\int AdV = \text{constant}$, and we assume $\hat{\omega}$ is constant within the packet such that the final energy of the short wave after the interaction is $E_{final}/E_{initial} = \hat{\omega}/\hat{\omega}_0$. Within the mid-frequency approximation the intrinsic frequency is inversely related to the vertical wavenumber of the short wave and thus decreases in vertical wavenumber result in increases in energy. The three dimensional ray path is shown in Fig.2. Since $l = 0$ the changes in the y -direction are due only to motion of the background inertial wave in the y -direction. The ray never reaches a critical level, even when the value of the horizontal phase speed is reached and surpassed because the phases of the inertial wave continue to propagate through.

Short waves with phase speeds less than the maximum horizontal velocity of the inertial wave are affected similarly. The main difference is the amount of time spent approaching the critical level depending on

the relationship between U_0 and c_{px} . Waves with initial vertical group speeds of 0.1m/s, 0.8m/s, and 3m/s, and horizontal phase speeds of 2.7m/s, 4.9m/s, and 9.5m/s respectively are shown in Fig.3. The slowest waves do not propagate as far in the x - or y - directions, but the relationship between the short wave interacting with an inertial wave and its counterpart which does not interact, is the same for each wave. The interacting wave slows as it approaches a critical level and therefore does not propagate as far vertically as its counterpart, but due to the eastward velocity of the inertial wave while it is traveling more slowly it propagates farther to the east. The greatest disparity between final horizontal locations occurs with the smaller scale, slower waves, where here the slowest wave is shifted about 400km and the fastest only 10km.

Short waves with a horizontal phase speed in the negative direction, traveling westward, approach critical levels 180° out of phase of those traveling in the positive- x direction. Again, there is no net transfer of energy or wave breaking necessarily as the basic situation is identical to that already shown. These waves, however, will have a final location hundreds of kilometers west of where they would be without an inertial wave present. This final location shift is opposite of the shift for eastward traveling waves.

When waves are propagating opposite to the propagation of the inertial wave caustics are reached (Vanderhoff et al. (2008), Broutman, Macaskill, McIntyre, and Rottman (1997)) due to the singularity when the group speed of the inertial wave is equal to the phase speed of the large wave. This only occurs when their vertical group speeds are in opposite directions. When the waves have group speeds in the same direction the result is these moving critical levels.

Vertical wavelength and wavenumber statistics for 1000 short waves is shown in Fig.4. All of the waves start with the same steepness, $\zeta_{z0} = 0.1$. Most of the short waves exit with the same parameters they entered the inertial wave interaction with, they are on the $m_f = m_i$ line. Those waves which are most likely to break are the waves with initially large vertical wavelength. This may be due to the initialization which is such that $\zeta_{z0} = m * \text{zeta}_{a0} = 0.1$ for each short wave, so short waves with small m_0 will have large initial amplitude.

b. Ray tracing through an inertial wave and background wind

When a background wind is introduced in addition to the inertial wave then a critical level can be reached. The background wind is a steady shear which starts at 0m/s at $2.5L$ below the center of the inertial wave and extends upward for 50 km with a maximum horizon-

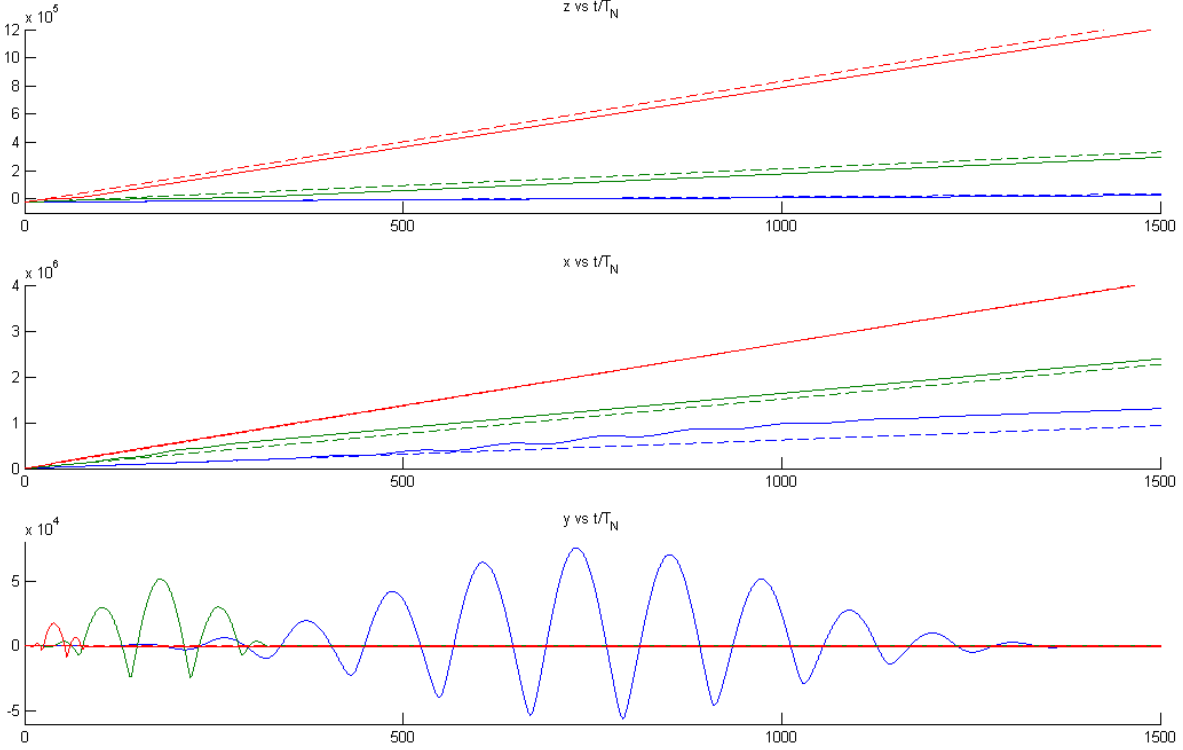


FIG. 3. Short waves with initial vertical group speeds of 0.1m/s, 0.8m/s, and 3m/s, and horizontal phase speeds of 2.7m/s, 4.9m/s, and 9.5m/s corresponding to the blue, green and red lines respectively. The dashed line represents the short wave which does not encounter an inertial wave. Ray path in $z - t$ space (top plot), $x - t$ space (middle), and $y - t$ space (lower). Notice the changes in y are only due to the inertial wave, no critical level is approached.

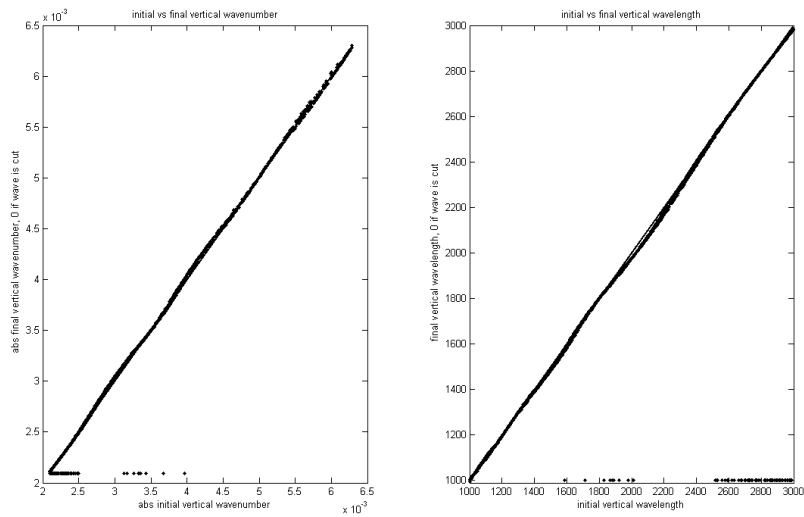


FIG. 4. Statistics of 1000 short waves propagating through an inertial wave. Solid line is where $m_f = m_i$. Waves with a final steepness normalized by initial steepness of 10 ($\zeta_{z0} = 0.1$) are cut from the calculations, and shown as having a final vertical wavenumber and wavelength of 0. Left plot is vertical wavenumber and right is vertical wavelength. Mainly waves of large vertical wavelength reach a large steepness and are cut.

tal velocity going eastward of 50m/s. The north-south background velocity is purely due to the inertial wave. Here the short waves have an initial vertical wavenumber $m = 2\pi/10000\text{m}$ such that the horizontal phase speed is 22m/s (note the midfrequency approximation cannot be used for these scales). The previous short waves used in the pure inertial wave interaction reach a critical level almost immediately in this setup because of their low horizontal phase speed.

Equivalent figures are shown when short waves approach an inertial wave while a background shear is also present. The ray path, steepness and vertical wavenumber are shown in Fig.5. In this case a critical layer is continually approached due to the horizontal velocity of the steady background shear. As the ray flattens out in $z - t$ space it is approaching a critical layer, and it continues to when the steady background velocity is equal to the horizontal phase speed of the short wave. The wave steepness decreases as the critical layer is continually approached as the absolute value of the vertical wavenumber increases. The wave may be spread by the interactions with the inertial wave before the critical level is approached, resulting in a drop in amplitude just before the critical level. Yet in the steady background shear case the short waves have an increasing amplitude as the critical level is approached, as is expected for a steady shear interaction. The vertical wavenumber continues to decrease as the critical layer is approached, but for the propagation through both the inertial wave and the steady shear, has some changes as the phases of the inertial wave continue to propagate through.

Fig.6 shows the ray path in three dimensions, showing the critical level is reached as the short wave continues to propagate in the $x-$ and $y-$ directions. This shows continual motion in the east-west propagation due to the steady shear background and oscillations in the north-south propagation due to the inertial wave. These oscillations in the north-south propagation of the wave would cease as the inertial wave propagates upward. The horizontal oscillations are significant, though, as Fig.6 shows the oscillations in the $y-$ direction have a 100km swing. This could result in wave breaking 50km north or south of the estimated location for waves propagating only through a steady shear wind.

Short wave propagation through a steady critical level, inertial wave only, and steady shear with inertial wave present are each very different. Only very small vertical scale short waves will be affected by a pure inertial wave with maximum horizontal velocity of 10 m/s. Since the background wind is stronger, larger scale waves will be affected by the interaction.

It seems for the general propagation direction, when an inertial wave is present there is a small change in vertical propagation as the inertial wave phases propagate through. The final approach to the critical level is the same and the short waves reach the same height. The main differences are in the final horizontal shift in wave location and the continual changing of the vertical wavenumber due to the inertial wave motions. These motions are continuous in this calculation because of their null group speed, but as they do have a slow vertical group speed eventually these oscillations in vertical wavenumber and horizontal location would die out as the inertial wave propagates upward through the shear.

When a number of short waves are traced through the inertial wave with a steady background shear present, and the short wave horizontal group speed is the same direction as the background velocity, all the waves with a horizontal phase speed less than the maximum steady background velocity will approach a critical level. These waves, if allowed to propagate, slowly become smaller and smaller, until their vertical wavelengths are less than one meter. These waves interact as would be expected with a critical layer, except with a few minor oscillations before the critical level due to the inertial wave. Waves which do not reach a critical level have their original properties, but have been advected in the direction of the wind.

Propagation opposite to the direction of the steady background results in turning points for the short waves. These waves' vertical wavenumber will change sign and the waves turn back on themselves. The horizontal wavenumber will stay constant and total reflection is expected, as Phillips (1977) found within the WKB approximation. Fig.7, and Fig.8 show short waves of vertical wavelength $m = 2\pi/10000\text{m}$ with a negative horizontal wavenumber, $k = -2\pi/10000\text{m}$ ($\hat{\omega} = 0.0141/\text{s}$). These waves are reflected when their horizontal group speed goes to zero, resulting in a frequency which approaches the buoyancy frequency, which occurs when $U_{steady} = -c_{gx} = 22\text{m/s}$. These waves are no longer followed as they are now trapped between the turning level and the ground because their horizontal wavenumber will not change sign and thus will always be propagating opposite the direction of the steady wind shear. The wave steepness decreases when approaching the turning point, then in the steady case increases back to its original value.

c. Numerical simulations through an inertial wave

Fully nonlinear numerical simulations show the two dimensional interaction with an inertial wave. Fig.9a is the perturbation density of a short wave with $m =$

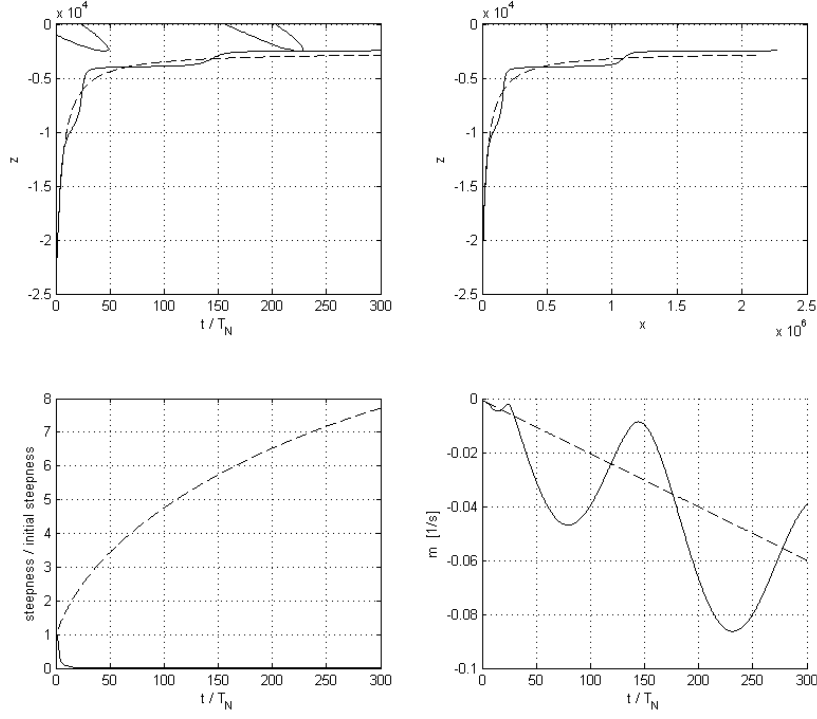


FIG. 5. Short wave with horizontal phase speed 22m/s. Plots as in Fig.1, where the elliptical regions in the upper left plot are outlines of critical layer values and the solid line represents the ray path when both a steady shear and inertial wave are present and the dashed line represents the ray path if only the steady shear is present. Both lines approach the same critical level.

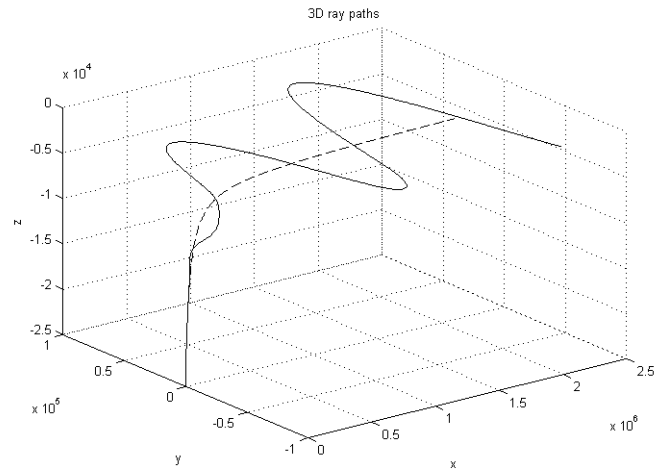


FIG. 6. Short wave with horizontal phase speed 22m/s. Ray path in $x - y - z$ space. Solid line is interaction with both inertial wave and steady shear, dashed line is for steady shear background only.

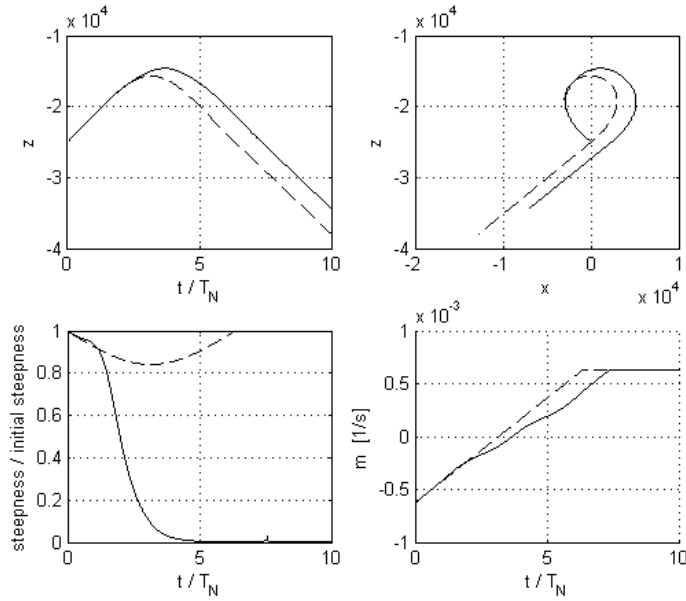


FIG. 7. As in Fig.5, but with short wave horizontal phase speed -22m/s . The ray reaches a turning point where the background steady velocity is 22m/s .

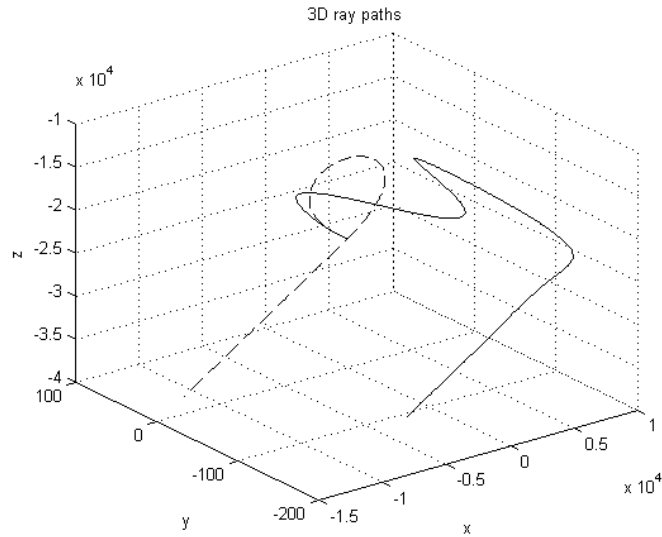


FIG. 8. Short wave with horizontal phase speed -22m/s . Ray path in $x - y - z$ space. Solid line is interaction with both inertial wave and steady shear, dashed line is for steady shear background only.

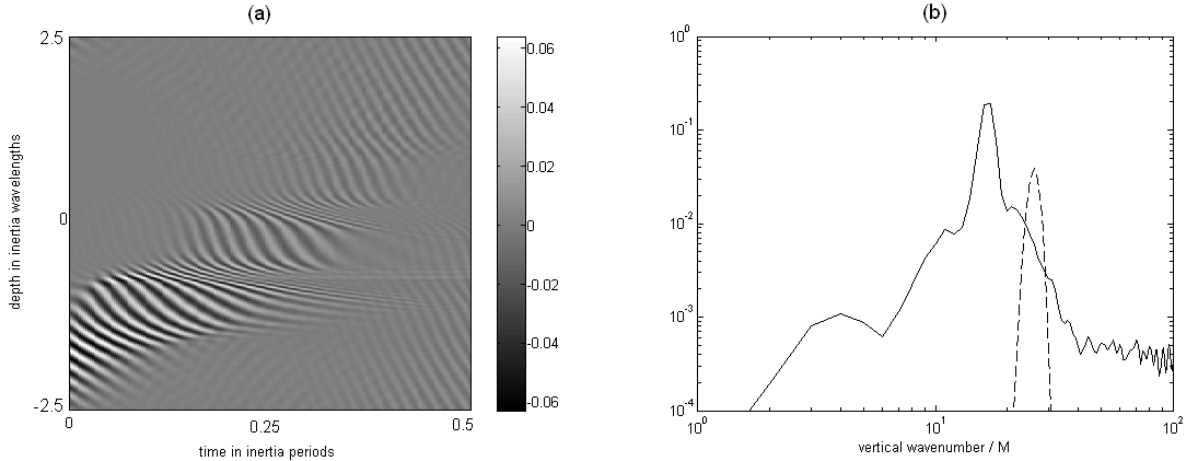


FIG. 9. Numerical simulation of short wave interaction with an inertial wave. (a) Perturbation density of short wave with $m_z = 2\pi/2000$. (b) Initial (dashed) and final (solid) vertical wavenumber spectrum.

$2\pi/10000\text{m}$ propagating upward through an inertial wave. The inertial wave cannot be seen in the density perturbation plot because it does not have an associated density perturbation. As in the ray tracing the short wave approaches a critical layer then goes back to original conditions as the critical level passes. It also loses amplitude as it propagates as it has spread. The steepness of this calculation actually exceeds unity for a short period of time while the wave approaches a critical level. A small jump was seen in the ray tracing at the same time, but of a much smaller magnitude. Fig.9b is the initial and final vertical wavenumber spectrum, averaged over the last quarter of the interaction. The initial spectrum is spread due to the packeting of the short wave. The final spectrum is peaked a little lower than the initial vertical wavenumber due to the increase in vertical group speed over the inertial wave. There is also some small spreading to higher and lower vertical wavenumbers due to the interaction.

The wave path generated by ray tracing matches that calculated through fully nonlinear simulations quite well. The approach to and retreat from the critical level is captured and only a small shift in vertical wavenumber is seen. Also, the overall spreading of the short wave is seen. However, the horizontal shift of the short wave cannot be tested because the simulations are only two-dimensional, and with periodic boundary conditions in the horizontal with a scale equal to that of one short wave horizontal wavelength, the horizontal shift is not calculated. Also, there is a strong increase in steepness that was not seen in the ray tracing.

d. Numerical simulations through an inertial wave and background wind

When a steady shear profile is present the classic critical level is approached as shown in Fig.10. The wave is absorbed at the critical level, the amplitude decreases. The final vertical wavenumber spectrum has a peak at a higher vertical wavenumber consistent with slower vertical propagation of the short wave. The steepness in this calculation never increases above the initial steepness, as was also seen in the ray tracing.

When an inertial wave is also in the background, as shown in Fig.11, the critical level is again reached, but by the time it reaches it the amplitude of the short wave has decreased significantly. This was also seen in the ray tracing. The short wave first interacts with the inertial wave, loses amplitude, spreads, and then approaches a critical level. Again there is a shift to higher vertical wavenumbers but because of the spreading due to the inertial wave it is not as clear as in the purely steady shear case. These interactions may result in the short wave losing energy before reaching the expected critical level when only a steady shear is present.

When the short wave is propagating in the opposite horizontal direction a turning point is reached, but is not well resolved by this model. Additional spreading of the short wave can be seen in the turning point when an inertial wave is also present, which was seen in the ray tracing as well.

Although the horizontal shift was not captured in the two-dimensional numerical simulations, they serve to verify the motion and wavenumber evolution of the interactions discussed as they match quite well, yet it is much more time efficient to use ray tracing to calculate

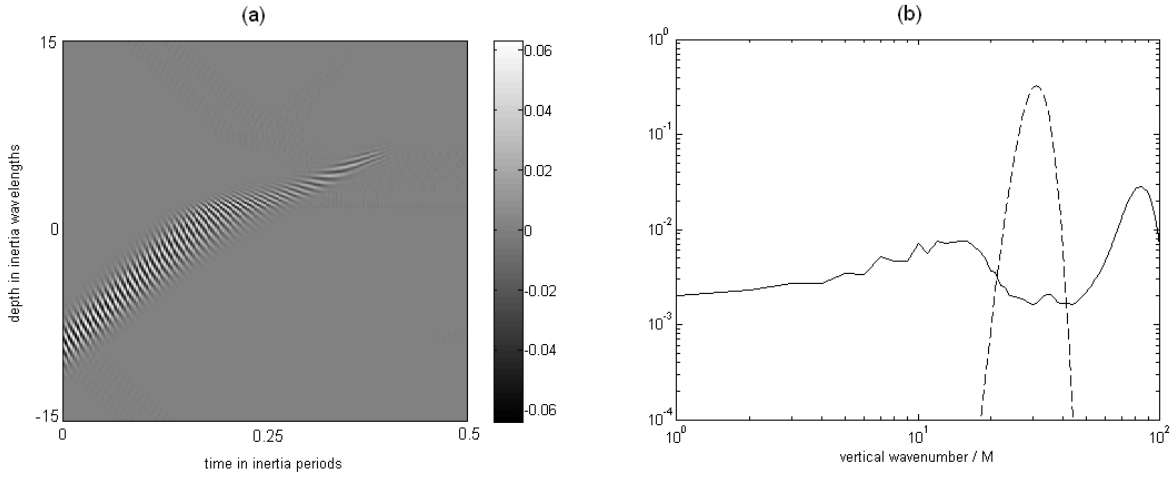


FIG. 10. Numerical simulation of short wave interaction with a steady background shear defined by equation 2 with $L = 10000\text{m}$ and $U_{max} = 50\text{m/s}$. (a) Perturbation density of short wave with $m_i = 2\pi/10000$. (b) Initial (dashed) and final (solid) vertical wavenumber spectrum.

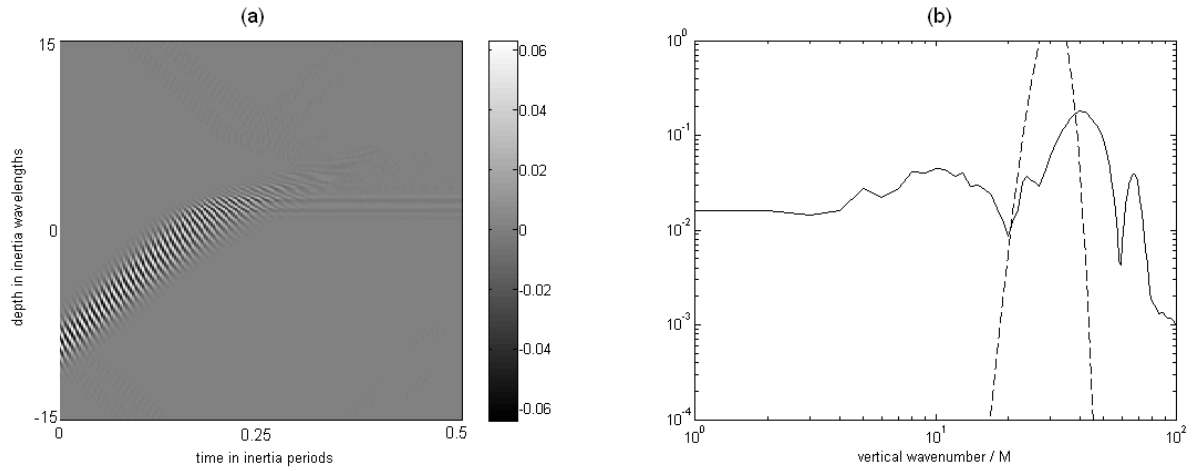


FIG. 11. Numerical simulation of short wave interaction with a steady background shear defined by equation 2 with $L = 10000\text{m}$ and $U_{max} = 50\text{m/s}$ with an inertial wave also present, centered with the shear. (a) Perturbation density of short wave with $m_i = 2\pi/10000$. (b) Initial (dashed) and final (solid) vertical wavenumber spectrum.

these motions.

4. Discussion

If the strongest winds are due to inertial waves with an upward group velocity than no critical level will be reached and short waves will continue to propagate after interacting with them with unchanged parameters. During the interaction with an upward propagating inertial wave, the short wave begins to reach a critical level, then rights itself as the critical level passes through with the phases of the inertial wave. Within the inertial wave the short wave properties change, and afterward the wavenumber spectrum has spread nearly equally both above and below the initial value, but still has a peak near the initial vertical wavenumber. Thus the spectrum of short waves propagating through an inertial wave are only altered while interacting. When an inertial wave is present the short waves will not reach as high a vertical location if given the same amount of time due to the slowing during the interaction. Short waves traveling to the west will be shifted further west, up to hundreds of kilometers, and waves traveling east will be shifted further to the east. The extent of this shift increases with decreasing horizontal phase speed. A relationship for this shift value in terms of wave parameters is being explored. Also, waves with larger vertical wavelengths may break. This may be an artifact due to the steepness being constant and therefore the amplitude of these waves is initially larger than smaller scale waves. In general the critical layer must be steady for an extensive amount of time for a short wave to break. There is also a possibility of the short wave breaking if the horizontal velocity of the inertial wave is large enough. This is being investigated.

Small scale waves with a horizontal phase speed component propagating with the wind, but less than the maximum wind will reach a critical level. When an inertial wave is also present these critical layer locations can be shifted tens of kilometers vertically and hundreds of kilometers horizontally. Also, due to the inertial wave interaction the short wave energy may be spread over a significantly larger volume before reaching a critical level. These waves will have a more broad final spectrum of vertical wavenumbers.

If the phase speed parallel to the wind is in the opposite direction of the wind, turning points will ensue. Again, the effect of the inertial wave's presence is to spread the energy of the short wave before turning so the short wave occupies a larger volume and afterward there is more of a spread of final vertical wavenumbers. Again both horizontal and vertical location shifts are seen.

If we know where short waves are initialized we can

calculate where they may break. This work has shown the importance of knowing if large scale inertial waves are present as they can act to significantly shift waves horizontally and even slightly vertically therefore shifting their breaking locations as well.

REFERENCES

- Balsley, B. B., and Carter, D. A., 1982: The spectrum of atmospheric velocity fluctuations at 8 and 86 km. *Geophys. Res. Lett.*, **9**, 465–468.
- Broutman, D., Macaskill, C., McIntyre, M. E., and Rottman, J. W., 1997: On doppler-spreading models of internal waves. *Geophys. Res. Lett.*, **24**, 2813–2816.
- Broutman, D., and Young, W. R., 1986: On the interaction of small-scale oceanic internal waves with near-inertial waves. *J. Fluid Mech.*, **166**, 341–358.
- Collins, R. L., Nomura, A., and Gardner, C. S., 1994: Gravity waves in the upper mesosphere over Antarctica: Lidar observations at the South Pole and Syowa. *J. Geophys. Res.*, **99**, 5475–5485.
- Dormand, J. R., and Prince, P. J., 1980: A family of embedded Runge-Kutta formulae. *J. Comp. Appl. Math.*, **6**, 19–26.
- Eckermann, S. D., 1997: Influence of wave propagation on the doppler spreading of atmospheric gravity waves. *J. Atmos. Sci.*, **54**, 2554–2573.
- Fritts, D. C., and Alexander, M. J., 2003: Gravity wave dynamics and effects in the middle atmosphere. *Rev. Geophys.*, **41**, 1003.
- Gardner, C. S., 1996: Testing theories of atmospheric gravity wave saturation and dissipation. *J. Atmos. Terr. Phys.*, **58**, 1575–1589, doi:10.1016/0021-9169(96)00027-X.
- Hamilton, K., and Mahlman, J., 1988: General circulation model simulation of the semiannual oscillation of the tropical middle atmosphere. *J. Atmos. Sci.*, **45**, 3212–3235.
- Heney, F. S., Wright, J., and Flatté, S. M., 1986: Energy and action flow through the internal wave field: an eikonal approach. *J. Geophys. Res.*, **91**, 8487–8495.
- Hitchman, M. H., Gille, J. C., Rodgers, C. D., and Grasseur, G., 1989: The separated polar winter stratopause: A gravity wave driven climatological feature. *J. Atmos. Sci.*, **46**, 410–422.
- Nakamura, T., Tsuda, T., Fukao, S., Kato, S., Manson, A. H., and Meek, C. E., 1993: Comparative observations of short-period gravity waves (10–100 min) in the mesosphere in 1989 by Saskatoon MF radar (52°n), Canada and the MU radar (35°n), Japan. *Radio Sci.*, **28**, 729–746.
- Phillips, O. M., 1977: *Dynamics of the Upper Ocean*, 2nd ed. Cambridge University Press.
- Sartelet, K. N., 2003a: Wave propagation inside an inertia wave. Part I: Role of time dependence and scale separation. *J. Atmos. Sci.*, **60**, 1433–1447.
- Sartelet, K. N., 2003b: Wave propagation inside an inertia

- wave. Part II: Wave breaking. *J. Atmos. Sci.*, **60**, 1448–1455.
- Sonmor, L. J., and Klaasen, G., 2000: Mechanisms of gravity wave focusing in the middle atmosphere. *J. Atmos. Sci.*, **57**, 493–510.
- Takahashi, M., Zhao, N., and Kumakura, T., 1997: Equatorial waves in a general circulation model simulating a quasi-biennial oscillations. *J. Meteor. Soc. Japan*, **75**, 529–539.
- Vanderhoff, J. C., Nomura, K. K., Rottman, J. W., and Macaskill, C., 2008: Doppler spreading of internal gravity waves by an inertia-wave packet. *J. Geophys. Res.*, **113**, C05018, doi:10.1029/2007JC004390.
- VanZandt, T. E., 1982: A universal spectrum of buoyancy waves in the atmosphere. *Geophys. Res. Lett.*, **9**, 575–578.
- Zhong, L., Sonmor, L. J., Manson, A. H., and Meek, C. E., 1995: The influence of time-dependent wind on gravity-wave propagation in the middle atmosphere. *Ann. Geophysicae*, **14**, 557–565.